Nonlinear Processes in Geophysics (2000) 7: 141–150

Nonlinear Processes in Geophysics

Kinetic simulations of the coupling between current instabilities and reconnection in thin current sheets

T. Wiegelmann and J. Büchner

Max-Planck-Institut für Aeronomie, Max-Planck-Str. 2, 37191 Katlenburg-Lindau, Germany
Fall 1999 also at STELAB, Nagoya University, Honohara 3-13, Toyokawa 442, Japan

Received: 21 December 1999 – Revised: 7 March 2000 – Accepted: 7 June 2000

Abstract. We investigate the coupling between current and tearing instability modes of a thin current sheet using the particle code GISMO. We identify pure tearing modes ($k_x \neq 0$), instabilities in the current flow direction ($k_y \neq 0$) and general 3D reconnection modes ($k_x \neq 0$ and $k_y \neq 0$). Our results give evidence that the coupling between tearing modes and current instabilities plays an important role for spontaneous magnetic reconnection. These modes give a substantial contribution to magnetic reconnection, additional to the well known 2D tearing mode. When allowing reconnection to occur in three spatial dimensions, a configuration, which was initially invariant in the current flow direction, develops into a configuration with no invariant direction.

1 Introduction

Spontaneous plasma instabilities play an important role in the dynamics of space plasmas. Initial small scale turbulence may cause an instability on macroscopic scales. It is especially important to know which instabilities lead to changes of the magnetic field topology and, therefore, allow reconnection. Magnetic reconnection (cf., e.g., Axford (1984); Biskamp (1993); Schindler et al. (1988); Vasyliūnas (1975)) is a process efficiently transforming magnetic field energy in plasmas. Magnetospheric substorms, for example, are assumed to be closely related to magnetic reconnection. The large scale structure of magnetic reconnection is well described in the framework of magnetohydrodynamics (MHD). Within MHD it is, however, necessary to make ad hoc assumptions about some nonideal transport processes. It is not possible to calculate these transport coefficients (resistivity) in the framework of MHD. In strictly ideal plasmas, on the other hand, the magnetic connection is conserved and magnetic reconnection as well as changes of the magnetic field topology are not possible. An ideal plasma in the strict sense, however, does not exist in nature. Thus, magnetic reconnection is possible in principle. Fundamental questions are: what causes nonideal effects in space plasma, of what kind are they and which consequences do they have for the reconnection process? These investigations cannot be carried out in the framework of MHD. Thus kinetic plasma simulations are necessary to obtain insight in the spatial and temporal scales of the dissipation processes. A basic understanding of these phenomena is required to obtain a better understanding of activity processes in space plasmas.

Recent research has shown that thin current sheets play an important role for the occurrence of reconnection. In situ observations of magnetospheric plasmas have proven the existence of these thin current sheets (Kaufmann, 1987; Mitchell et al., 1990; Pulkkinen et al., 1992; Sanny et al., 1994; Sergeev et al., 1990). Immediately before the occurrence of a geomagnetic substorm, the sheet width of current sheets is comparable with the ion gyroradius. Theoretical investigations (cf., e.g., Schindler and Birn (1993); Parker (1994); Wiegelmann and Schindler (1995)) showed that the formation of thin current sheets is typical for space plasmas. Current or gradient driven instabilities were assumed to occur in thin current sheets and the cause of anomalous resistivity in the plasma. The formation of these thin current sheets can be described in the framework of MHD. It is, however, not possible to investigate their further development in a fluid model.

A first step towards a better theoretical understanding of microphysics and dissipation in collisionless plasmas are hybrid simulations. Hybrid codes with massless electrons enable the study of the influence of the Hall effect and the acceleration of ion beams (Lottermoser and Scholer, 1997). In their approach it is, however, necessary to make ad hoc assumptions about the resistivity. Still with massless electrons Hesse et al. (1995) investigated how anisotropy in the pressure tensor influences collisionless magnetic reconnection. Later investigations (Hesse et al., 1998; Shay et al., 1998) took into account also electron inertia. For a consistent investigation of collisionless reconnection one has to consider, however, the electron effects fully kinetically. In order to cope with the huge particlenumbers, the Particle-

Correspondence to: T. Wiegelmann

In-Cell (PIC) method was developed (Birdsall and Langdon, 1991). A larger number of particles is combined to macro-particles. Reduced mass ratios are used to solve the technical problem of strongly differing time-scales of electron and ion motion. With new simulation techniques, one can investigate large mass ratios of electrons to ions. The essential physical differences between the mobility of the components can be described sufficiently well if the mass ratio reaches one order of magnitude.

Two-dimensional kinetic simulations of thin current sheets were carried out first in the direction perpendicular to the reconnection plane (Winske, 1981; Brackbill et al., 1994). They revealed mainly gradient instabilities at the edges of the current sheet which saturate at a relatively early stage. The further development as well as the disruption of the current sheet was not investigated by simulations at that time. Later, two-dimensional kinetic simulations in the reconnection direction where carried out (cf., e.g., Pritchett (1994); Pritchett and Büchner (1995) and references therein). They confirmed that a current sheet is stabilized by a finite normal component of the magnetic field accross the sheet. Theoretical contemplations had predicted this before (Galeev and Zelenyi, 1976; Lembége and Pellat, 1982). The reason for the stabilization is that a bigger quantity of free energy is necessary to compress the plasma rather than it is available from a tearing instability. This effect was confirmed in two-dimensional configurations. It was theoretically predicted that it could disappear in the transition to three dimensions (Büchner, 1995, 1996). Hence, the traditional limitation to two-dimensional systems may cause huge problems neglecting, e.g., the essential intrinsic three-dimensionality of the reconnection process (Büchner and Kuska, 1996; Pritchett et al., 1996; Büchner, 1999; Zhu and Winglee, 1996). In order to understand the situation, the three dimensional PIC code GISMO was developed (Kuska and Büchner, 1999). Both analytically and by kinetic simulations with GISMO have shown that current instabilities occur in thin current sheets and influence the magnetic reconnection process (Büchner and Kuska, 1999).

In this paper, we investigate the physics of this coupling process in some more detail. We present new results of computer simulations carried out with the help of GISMO. Since we want to obtain insights into the role of current instabilities for the magnetic reconnection process, we compare simulations with and without these current instabilities. The outline of the paper is as follows. In section 2 we repeat the basic equations and outline our simulation approach. In section 3 we present the differences in the reconnected magnetic field structure and the plasma density for both cases. In section 4.2 we investigate the role of the electric field for the coupling mechanism between the sausage instability and the magnetic reconnection process. We investigate the role of different modes by means of a two dimensional spatial Fourier analysis. In section 5 we summarize our results and give an outlook to future work.

2 Basic Equations and Simulation Approach

We describe the plasma by the collisionless Boltzmann equation (Vlasov equation):

$$\frac{\partial f_j}{\partial t} + \vec{v}\cdot\nabla f_j + \frac{q_j}{m_j}\left(\vec{E} + \frac{\vec{v}\times\vec{B}}{c}\right)\cdot\nabla_v f_j = 0 \qquad (1)$$

f_j stands for the distribution function, $\vec{v}$ for the velocity, q_j for the electric charge, m_j for the mass, $\vec{E}$ for the electric field, $\vec{B}$ for the magnetic field, c for the speed of light, t for the time and j is an index for the particle sort (electrons $= e$, ions $= i$). The relativistic equations of motion are given by:

$$\begin{aligned}
\frac{\partial v_x^*}{\partial \tau} &= \sqrt{1-v^{*2}}\left(F_x\,(1-v_x^{*2}) - F_y\,v_x^* v_y^* - F_z\,v_x^* v_z^*\right)\\
\frac{\partial v_y^*}{\partial \tau} &= \sqrt{1-v^{*2}}\left(-F_x\,v_x^* v_y^* + F_y\,(1-v_y^{*2}) - F_z\,v_y^* v_z^*\right)\\
\frac{\partial v_z^*}{\partial \tau} &= \sqrt{1-v^{*2}}\left(-F_x\,v_x^* v_z^* - F_y\,v_y^* v_z^* + F_z\,(1-v_z^{*2})\right)
\end{aligned}$$

where the Lorentz force is given by $\vec{F} = \frac{q}{mc^2}\left(\vec{E} + \vec{v}^* \times \vec{B}\right)$, $\vec{v}^* = \vec{v}/c$ and $\tau = lt/c$. Here, l is the maximal box dimension $l = \max(l_x, l_y, l_z)$.

These equations have to be solved selfconsistently with the wave equations for electrostatic potential ϕ and magnetic vectorpotential $\vec{A}$.

$$\Delta\phi - \frac{1}{c^2}\frac{\partial^2\phi}{\partial t^2} = -4\pi\varrho \qquad (2)$$

$$\Delta\vec{A} - \frac{1}{c^2}\frac{\partial^2\vec{A}}{\partial t^2} = -4\pi\vec{j} \qquad (3)$$

$$\frac{1}{c}\frac{\partial\phi}{\partial t} + \vec{\nabla}\vec{A} = 0 \qquad (4)$$

Here ϱ stands for the charge density and $\vec{j}$ for the current density. We use the particle in cell code GISMO to solve these equations (Kuska and Büchner, 1999). As a first step we describe the magnetic field structures with a Harris sheet profile (Harris, 1962).

$$f_j(\vec{r},\vec{v}) = \frac{n_j(z)}{\pi^{3/2}v_{tj}^3}\cdot\exp\left(-\frac{m_j}{2k_B T_j}(v_x^2 + (v_y - u_{dyj})^2 + v_z^2)\right)$$

where $n_j(z) = n_0\cdot\cosh^{-2}\left(\frac{z}{L_z}\right)$ for both electrons and protons and $L_z = \sqrt{\frac{k_B\cdot(T_e+T_i)}{2\pi n_0 e^2}}\cdot\frac{c}{u_{di}-u_{de}}$

In this paper n stands for the particle density, L_z for the sheet half width, v_{tj} for the thermal velocity, k_B for the Boltzmann constant, T_j for the temperature, e for the elementary charge and u_{dyj} for the drift velocity. The index j stands for ions (i) and electrons (e).

We investigate a marginally thin current sheet, where the sheet half width L_z is of the order of the ion gyro radius. The gyro frequency is $\Omega_{cj} = \frac{eB_0}{m_j c}$ and the gyro radius $r_j = \frac{v_{Tj}}{\Omega_{cj}}$. In a Harris sheet, the Larmor radius in the ambient field

is half of the inertial length $\lambda_j = \frac{c}{\Omega_{pj}}$, where Ω_{pj} is the plasma frequency. Consequently the full sheet width of $2L_z$ approaches the ion inertial length for $r_i = L_z$. Within kinetic plasma simulations we also have to resolve the Debye length $\lambda_D = \sqrt{k_b T_j / 4\pi n_0 e^2}$, where n_0 is the maximum particle density. Electric fields vanish in a Harris sheet for $\frac{u_{de}}{u_{di}} = -\frac{T_e}{T_i}$.

The wave equation for the electromagnetic field is solved on a equidistant grid with $64 \times 64 \times 64$ grid points. The box length corresponds to $12L_z = 6\lambda_i$ in each direction. Thus one sheet width $\lambda_i = 2L_z$ is resolved by 12 grid points. For numerical reasons, we have to resolve the Debye length and thus we obtain additional technical restrictions for choosing a suitable parameter set. The relativistic equations of motion are solved for 2 million particles. In the x and y direction we use periodic boundary conditions and in the z direction we set the electric ϕ and magnetic A potential to zero.

3 Simulation Results

We present results for the following set of parameters: $T_i = 10keV$, $T_e = 5keV$, $m_i/m_e = 4$. Within this parameter set the ion Debye length is resolved by 1.5 grid points and the electron Debye length with 1.0 grid point. [1] The initial thermal velocities are $\frac{v_{Ti}}{c} = 0.14$ and $\frac{v_{Te}}{c} = 0.20$. We resolve the ion gyroperiod with approximately 50 integration time steps and the electron gyroperiod with 12 integration time steps. The equilibrium Harris sheet magnetic field lines are in the x-direction and z points in the direction of the pressure gradient. y is the direction of current flow.

The aim of this contribution is to obtain some insight about magnetic reconnection in three dimensional systems. While the magnetic field and plasma parameters are initially invariant in the y-direction ($\frac{\partial}{\partial y} = 0$), they can become structured in the y-direction during the evolution. Drift current instabilities are supposed to play a major role for these structuring in the y-direction and thus for magnetic reconnection in three dimensions. In the absence of electrostatic fields a drift current instability can no longer be supported. Thus one can suppress drift current instabilities by enforcing $\nabla\phi = 0$. To investigate the role of current instabilities (and thus electrostatic fields) we carried out two simulation runs with the same parameter set (see above), except in one of the runs (case A) we neglected the static part of the electric field. ($\vec{E} = -\frac{1}{c}\frac{\partial \vec{A}}{\partial t} - \nabla\phi$) and the $(-\nabla\phi)$ term is neglected in case A while we consider it in case B. We are aware of the fact that it is not possible to switch off the electrostatic field in nature, but to do that in the simulations is a suitable method to investigate its role for the reconnection process.

In figure 1 we present the magnetic field lines for both simulations after magnetic reconnection occure. Note, that the reconnection process is faster in full three dimensions (case B) and thus both pictures are snapshots at different times. The upper panel in figure 1 shows the field lines at $t\,\Omega_{ci} = 9.2$ for case A and the lower picture shows the magnetic field lines at $t\,\Omega_{ci} = 7.0$ for case B. In the upper panel we do not see any structuring in the y-direction and the plasmoids formed as a consequence of magnetic reconnection are concentrated in the classical 2D xz-reconnection-plane. Thus, magnetic reconnection without electrostatic fields (and thus without kinetic current instabilities) in three dimensions is very similar to reconnection in two dimensions.

A completely different evolution of the magnetic field lines happens if $(-\nabla\phi)$ is taken into account (lower panel of figure 1). The reconnected magnetic field lines are not invariant perpendicular to the classical xz-reconnection plane any more, but show fully three dimensional structure. Figure 2 shows a blow-up of part of figure 1 lower panel. It shows some details of the structure. The invariance in y-direction, which has been observed for simulations without electrostatic field (case A) is no longer present. The additional structuring is not only visible in the magnetic field, but also in the density profile. We show the ion density profile in figure 3. The density profile for the simulation without static electric field in the upper picture is approximately the initial Harris sheet profile and we only see a smooth bending as a consequence of magnetic reconnection. In the lower picture, for the simulation with electrostatic field, however we see a strong structuring of the density profile in the current direction (y). The profile is no longer a Harris sheet anymore, but an instability in the current direction has happened. The instability is symmetric in z. It was called kinetic sausage instability (Büchner and Kuska, 1999). But in general, a current instability can be either a drift kink instability (DKI) or a drift sausage instability (DSI). Let us remark that we observe a DKI instead of a DSI in simulations with lower mass ratios ($M_i/M_e = 1$ and $M_i/M_e = 2$). The evolution of a DKI in thin current sheets for low mass ratios has been also investigated by (Pritchett and Coroniti, 1996). These authors also found that with increasing mass ratio the growth rate of DKI decreases. (Zhu and Winglee, 1996) carried out simulations showing that magnetic reconnection and a DKI occur on the same timescale and the reconnected magnetic field gets a helical structure. Within the parameter regime investigated in the present contribution the drift current instability is a DSI.

Our simulations give evidence that current instabilities (DSI) and reconnection are directly coupled through the electrostatic field. We will undertake a step toward a better understanding of the coupling between current instabilities and magnetic reconnection.

4 Mode Structure of the fields

4.1 Magnetic field structure

To investigate the physics of the coupling between the different instabilities for three dimensional magnetic reconnection, we carried out a two dimensional Fourier analysis of the magnetic field component B_z in the xy-cross-section af-

[1] In explicit particle simulations one has to resolve the Debye length with at least ≈ 0.3 grid points (Birdsall and Langdon, 1991).

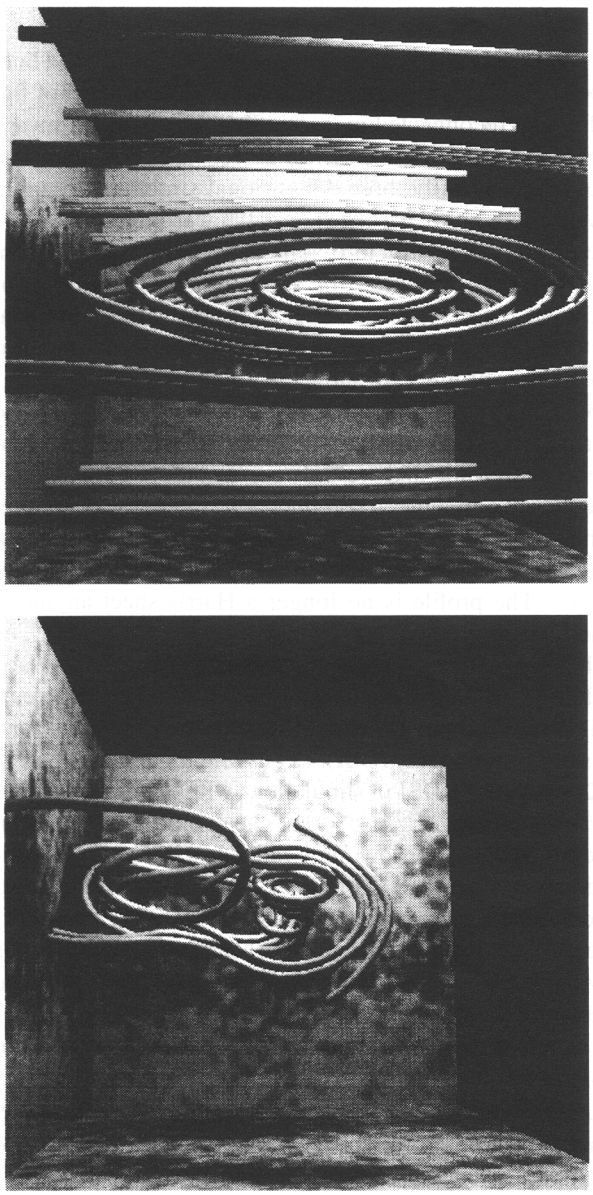

Fig. 1. Magnetic field lines after reconnection has occured. Upper panel case A for $t \cdot \Omega_{ci} = 9.2$ and lower panel case B for $t \cdot \Omega_{ci} = 7.0$. The back panels indicate the electron density structure in three cross-sections.

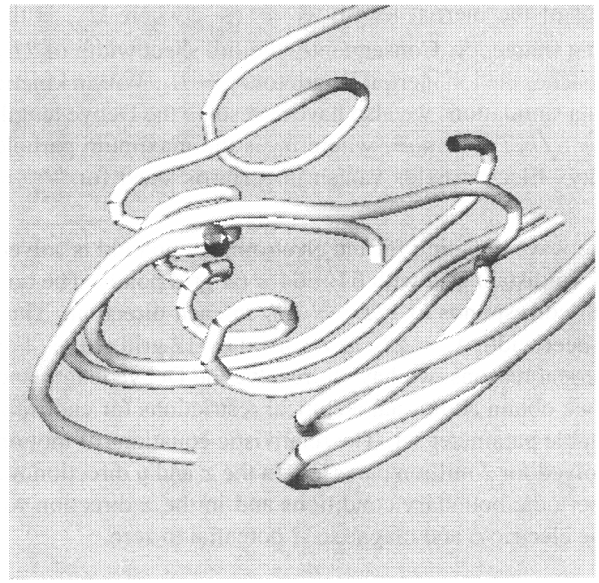

Fig. 2. Magnetic field lines after reconnection has occured for case B. This picture shows a blow-up of part of figure 1 lower panel to demonstrate the three dimensional structure of the magnetic field.

ter reconnection developed. We use the following definition for the Fourier modes

$$F(k_x\ k_y) = \left| \frac{1}{n} \sum_{r=0}^{n} \sum_{s=0}^{n} f(x,y) \exp\left(\frac{2\pi i}{n} (r\ \frac{x}{\lambda_i} + s\ \frac{y}{\lambda_i}) \right) \right|$$

where $f(x,y) = B_z(x,y,z=0)$ here. While the initial Harris sheet magnetic field has only a component in the x-direction, the development of a z-component during the evolution is a good indicator that magnetic reconnection has occured. We normalize the length scale to the ion inertial length λ_i and the Fourier modes by $k = \frac{2\pi}{\lambda_i}$. Fourier components with $(k_x > 0,\ k_y = 0)$ correspond to pure 2D tearing modes, modes with $(k_x = 0,\ k_y > 0)$ correspond to current instability and we call all other modes $(k_x > 0, k_y > 0)$ general 3D reconnection modes.

Figure 4 shows the mode structure for the simulations without a static electric field (case A) in the upper panel and for the simulation with allowing static electric field (case B) in the lower panel at the same times as in figures 1 (A and B). The results without static electric field show a clear domination of the $(k_x = 1, k_y = 0)$ tearing mode. All other modes are below the noise level. We use this classical 2D reconnection mode $(k_x = 1\ , k_y = 0)$ for normalization of the Fourier amplitudes. The consideration of $\nabla\phi \neq 0$ leads to a different mode structure (lower panel in figure 4). The $(k_x = 1, k_y = 0)$ tearing mode is present, too. But the $k_x = 1, k_y = 1$ general 3D reconnection mode is dominating. Additionally, a $k_x = 1, k_y = 2$ general 3D reconnection mode is present with a somewhat lower amplitude (about the same as the pure tearing mode). We also observe three modes with $k_x = 2$ (the pure tearing mode $(k_x = 2, k_y = 0)$ and the general 3D reconnection modes $(k_x = 2, k_y = 1)$ and

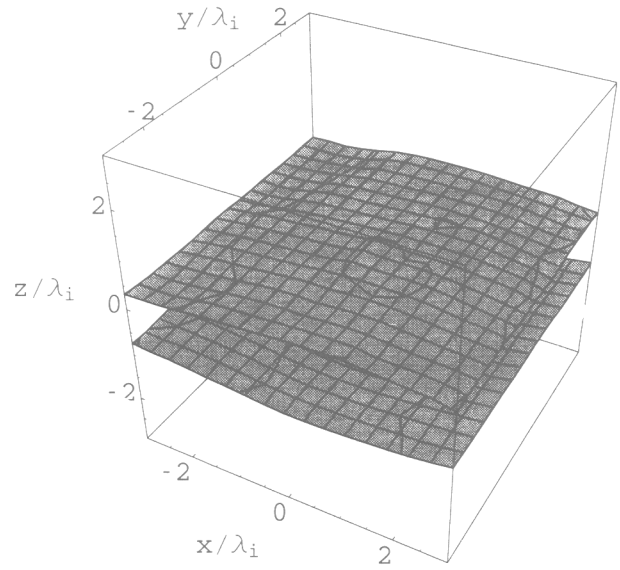

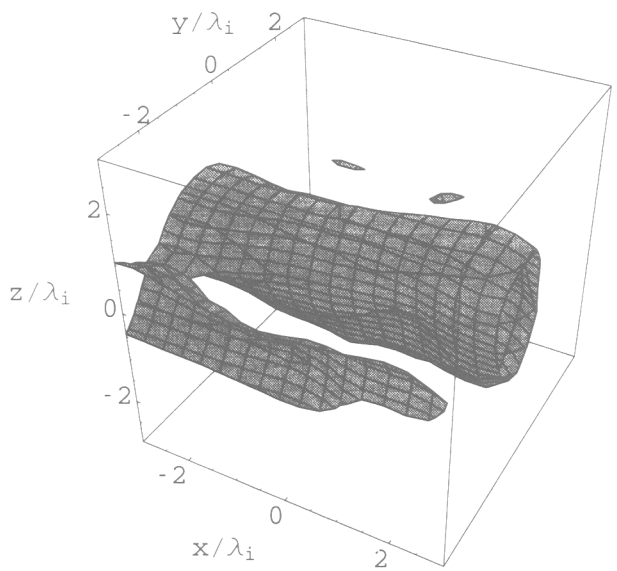

Fig. 3. 3D Surfaceplots of the ion density profile for simulations without static electric field in the upper panel and with a static electric field in the lower picture respectively. (Same times as in figure 1.)

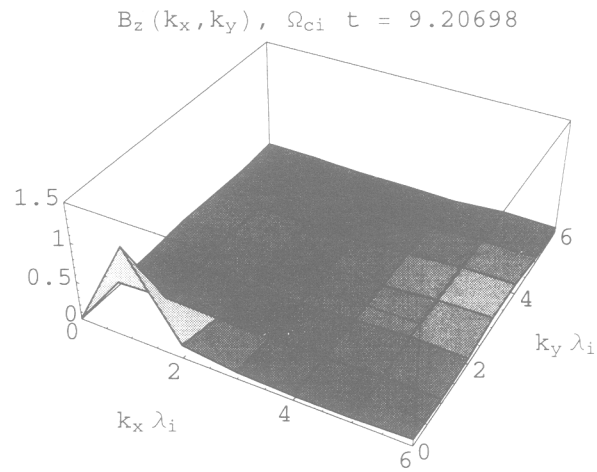

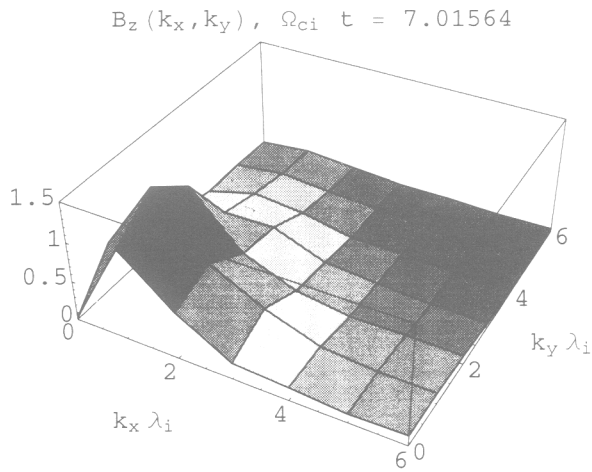

Fig. 4. Results of a two dimensional Fourier analysis with respect to the magnetic field B_z. The upper panel corresponds to case A and the lower panel to case B. The amplitudes are normalized to the maximum of the pure 2D tearing mode (the only relevant mode in case A).

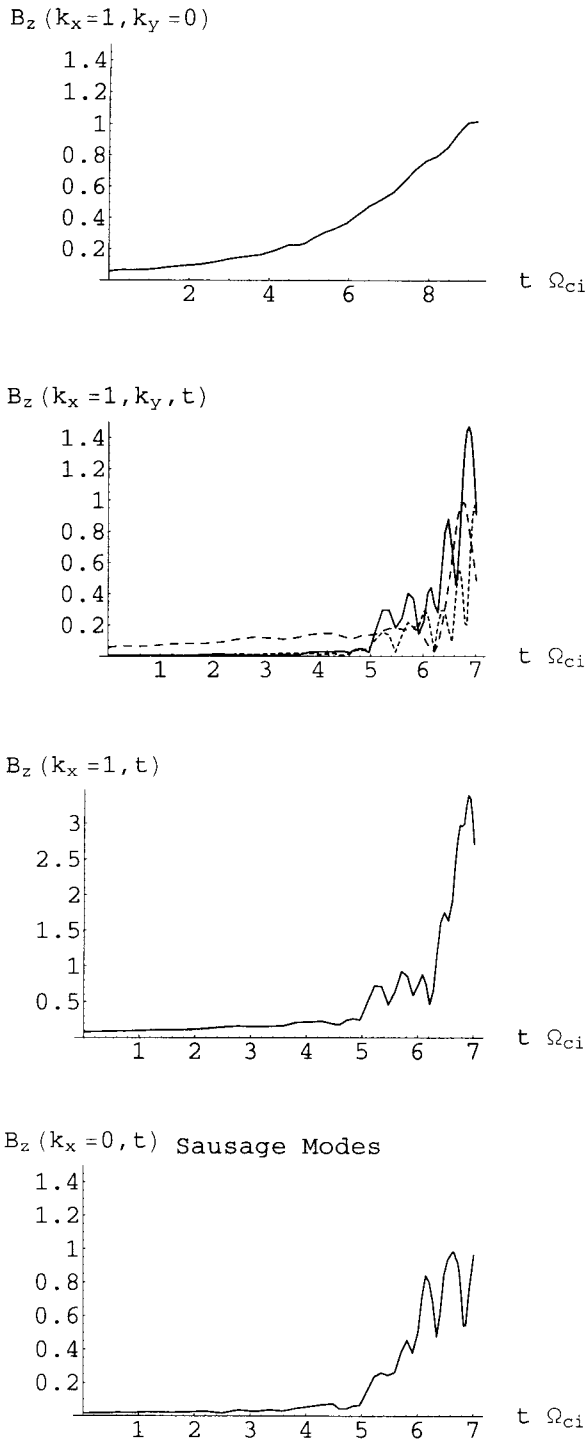

Fig. 5. Time evolution for different modes (Fourier amplitudes of B_z). The upper panel shows the pure tearing mode ($k_x = 1, k_y = 0$) for case A. (We use the maximum of this mode for normalization of all presented Fourier modes.) The third panel shows the most significant modes for case B. ((1,0) dashed, (1,1) solid line , (1,2) dotted respectively.) In the third picture we sum up these three most relevant modes. The lower picture corresponds to the sausage modes (case B)

($k_x = 2, k_y = 2$). The ($k_x = 2, k_y = 1$) has the highest amplitude of these three modes.) which are significantly lower than the ($k_x = 1$) modes. We conclude that both pure tearing instabilities and general modes play an important role for real 3D magnetic reconnection. The classical 2D reconnection tearing instability is present, too. It is, however, only one of several instabilities responsible for magnetic reconnection in 3D.

Let us now demonstrate the temporal evolution of the most significant unstable modes. Figure 5 depicts the time history for different modes. The upper picture corresponds to case A and shows the only relevant mode $k_x = 1, k_y = 0$. The other panels correspond to case B. In the second panel we present the three most important modes, the ($k_x = 1, k_y = 0$) pure tearing mode as a dashed line, the ($k_x = 1, k_y = 1$) general 3D reconnection mode as a solid line and the ($k_x = 1, k_y = 2$) general 3D reconnection mode as a dotted line. In the third panel we sum over the modes, which all together give a main contribution to the reconnection rate. While at times before $t\Omega_{ci} = 5.0$ the reconnection rate for both simulation runs is very similar and dominated by the pure tearing mode in both cases, later in time the reconnection rate for case B becomes significantly higher as a result of the occurrence of general 3D reconnection modes. Note that the oscillations in the growth rate correspond to the lower hybrid frequency $\Omega_{hybrid} = \sqrt{\Omega_{ci}\Omega_{ce}}$. In the lower panel we sum up over all relevant sausage modes ($k_y \leq 6$). The different mode structure in case A and case B, respectively and the faster reconnection process gives evidence that magnetic reconnection is not driven only by a pure tearing mode in three dimensions. Not allowing electrostatic fields, as we did for our investigations (in case A), is of course not possible in nature. Here, electrostatic phenomena are always present and influence the reconnection process. We investigate the role of electric fields for three dimensional magnetic reconnection in the next section.

4.2 Mode structure the electric field

We now investigate the electric field. In case A we did not allow electrostatic fields and so we concentrate our investigations to case B here. We demonstrate the evolution of the E_y component of the electric field in the xy-plane at the center of the current sheet at $z = 0$ since we can identify in this way both the current- and the tearing modes. Figure 6 shows snapshots of $E_y(x, y, z = 0)$ taken at different times. We observe the evolution of small scale fluctuations structuring the electric field in the y-direction. These fluctuations increase and lead finally to a large scale structuring of the electric field in the y-direction. This coincides with the formation of sausages in the ion and electron density. Later in time we also observe an overlaying structuring in the reconnection direction(x). The amplitude of the reconnection E_y component is smaller than the electrostatic field of the current instability. We want to point out that we observe a sausage instability and not a kink instability. A kink instability would be anti-symmetric in the electric field with respect

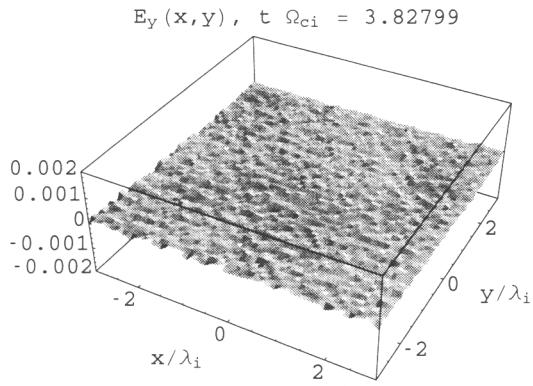

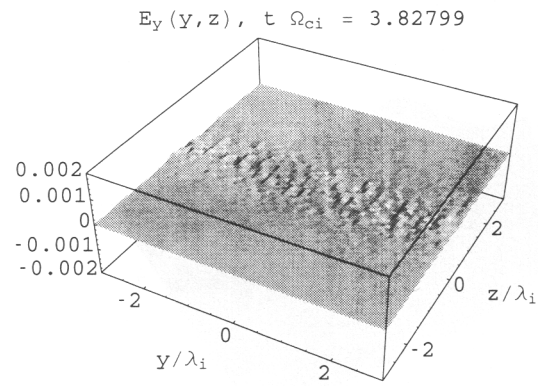

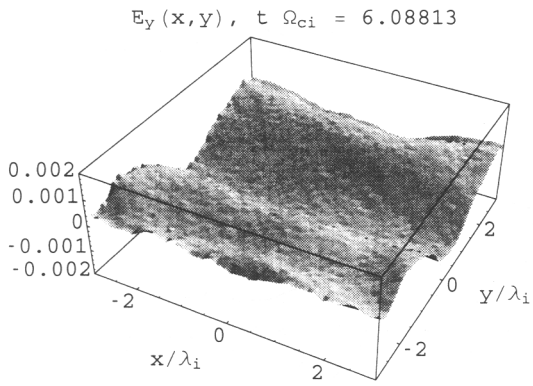

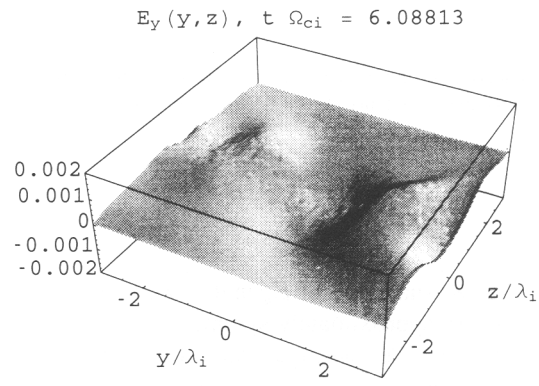

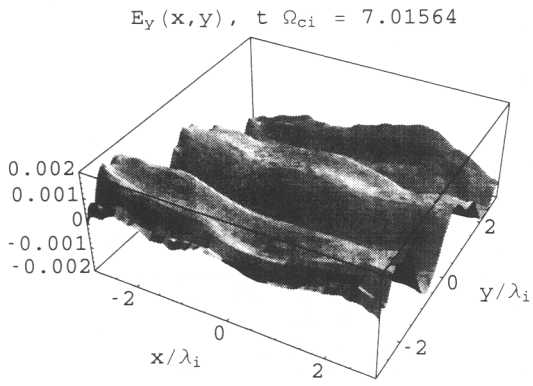

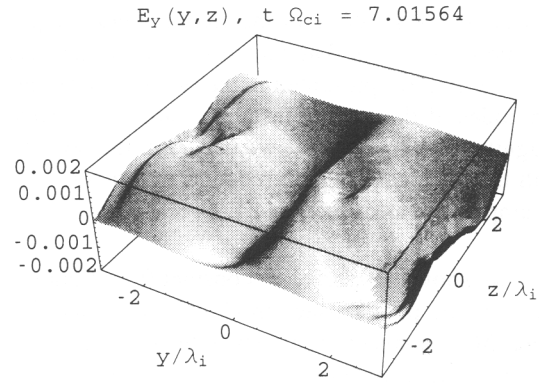

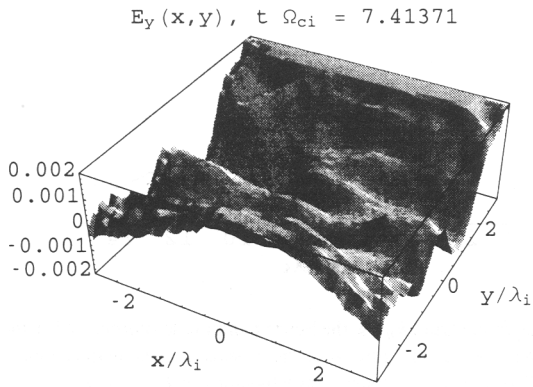

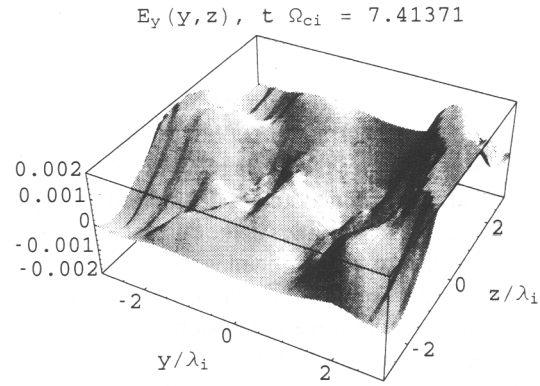

Fig. 6. Snapshots regarding the time evolution of E_y (case B) in the xy-cross-section.

Fig. 7. Snapshots regarding the time evolution of E_y (case B) in the yz-cross-section.

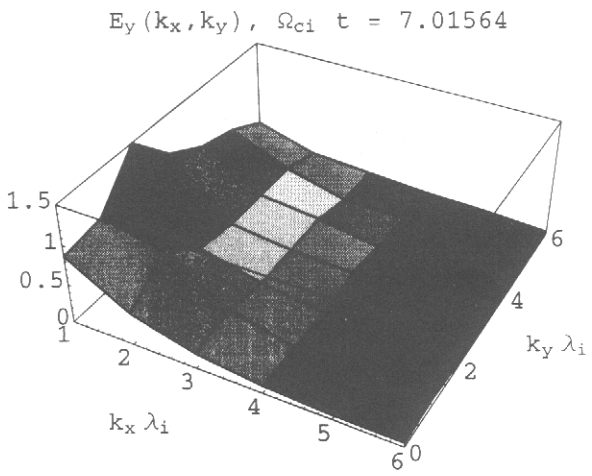

Fig. 8. Fourier modes for the electric field E_y (case B) after removing the pure sausage mode components ($k_x = 0$) whose amplitude dominates absolutely.

to z. Figure 7 shows snapshots of E_y in the yz-plane ($x = 0$) and one can see an approximately symmetric behaviour of E_y with respect to z. We investigate the different modes of E_y with help of a two dimensional Fourier analysis in the xy-plane at the center of the current sheet. Figure 8 shows a snapshots of the mode structure of the electric field component E_y at time $t\Omega_{ci} = 7.0$. The pictures correspond to the same time as the pictures presented in the previous sections. As the amplitudes of the tearing instability are of the same order of magnitude in E_y and B_z, we use the same normalization (with the classical 2D pure reconnection mode.) for the Fourier amplitudes as in section 4.1.

In figure 9 we show cuts for k_x = constant from figure 8. The panels show the pure sausage mode ($k_x = 0$) and different general 3D reconnection modes with fixed values of x ($k_x = 1,\ 2,\ 3$) as a function of k_y. The sausage modes dominate in the E_y component and the $k_y = 1$ and the $k_y = 2$ sausage mode have the highest amplitude. It is remarkable that the wavelength in the current direction (k_y) of the most significant general 3D reconnection modes ($\{k_x, k_y\} = \{1,2\},\ \{1,1\},\ \{2,1\}$) coincide with the wavelength of the pure sausage modes in the current direction. Magnetic reconnection starts somewhat after the sausage mode and the corresponding general 3D reconnection modes become present. This gives evidence that instabilities in the current flow direction might be important to trigger the magnetic reconnection process and general 3D reconnection modes play an important role for reconnection in three dimensional systems. The magnetic reconnection process is not limited to the classical xz-reconnection plane. Due to the general 3D reconnection modes, the magnetic field also gets structured in the current direction, which leads to a three dimensional structure of the magnetic field lines.

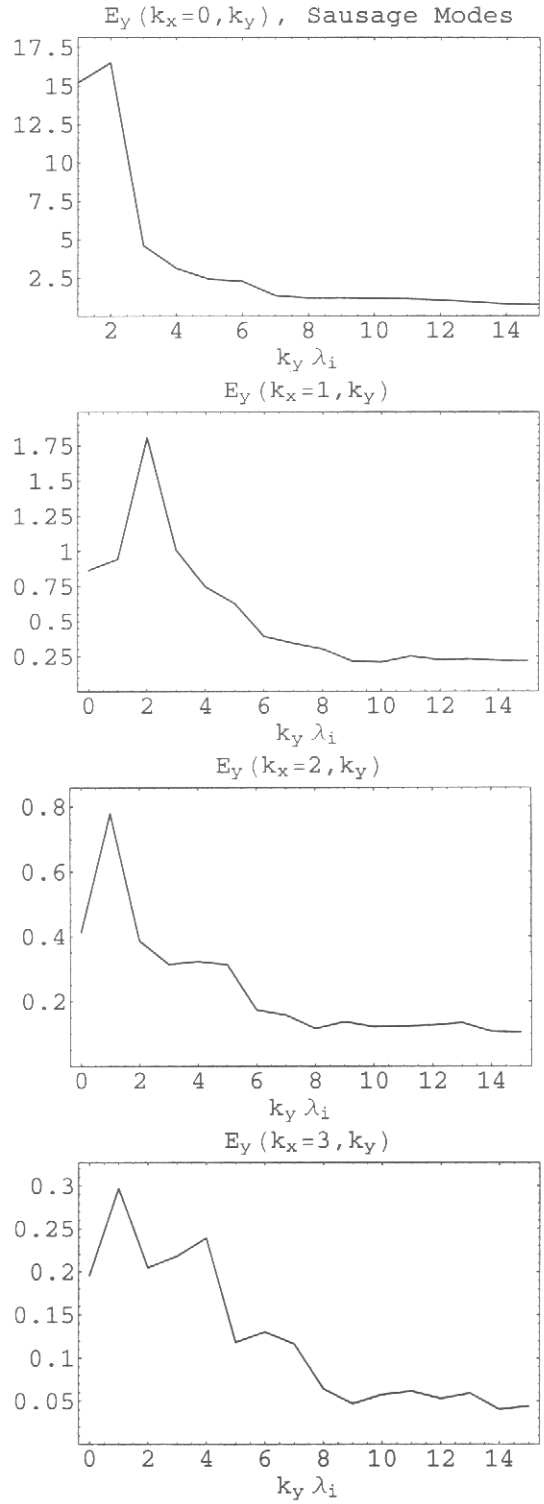

Fig. 9. 2D Fourier spectrum k_y vs. the Fourier amplitude (normalized to the classical tearing mode as in figure 4) of the sausage modes, tearing modes and general 3D reconnection modes. (Investigations of E_y, case B)

5 Conclusions

We undertook a step toward a better understanding of the coupling between current instabilities and magnetic reconnection. The evolution of a kinetic sausage instability has been investigated both analytically and numerically in (Büchner and Kuska, 1999). This bulk current instability correlate the small scale turbulence (Büchner, 1998). As an open question remained, how concrete this instability couples to magnetic reconnection. In the framework of this work we found that reconnection through thin current sheets directly couples with the electrostatic perturbations of the current instabilities. If one neglects the electrostatic field magnetic reconnection becomes similar to two dimensional tearing and a kinetic current instability cannot occur. We have verified this fact by enforcing $\nabla\phi = 0$. In nature, however, thin current sheets cause electrostatic fluctuations due to current instabilities. This leads to a faster evolution of the magnetic reconnection process. The current instabilities also determine the structure of the reconnected magnetic field. We conclude that, therefore, reconnection through thin current sheets is not only due to a pure tearing instability, but additional due to a general mode, which evolves oblique to the pure tearing modes and the pure sausage modes. In the current direction the resulting mode has the same wavelength as the pure sausage modes. Due to the current instability the reconnected magnetic field becomes structured in the current direction. The magnetic field contains a component in the current direction causing a three dimensional structure of magnetic reconnection (Büchner, 1999). Our results gives evidence, that a direct coupling between tearing and current instability dominates magnetic reconnection process through thin current sheets.

Additional research is necessary to enlighten the importance of current or other kinetic instabilities for the reconnection process in dependence on different initial situations. A next step is, for example, to investigate whether magnetic shear or a normal component in the equilibrium magnetic field influences the nonlinear mode coupling.

Acknowledgements. We thank Jens-Peer Kuska for developing the PIC code GISMO and Andreas Kopp, Bernd Nikutowski and Antonius Otto for useful discussions. This work was supported by the Deutschen Zentrum für Luft und Raumfahrt, Project: 50 OM97012.

References

Axford, W.I., Magnetic field reconnection, in *Reconnection in space and Laboratory Plasma*, ed. by E.W. Hones Jr., pp. 4-14, Geophysical Monograph 30, AGU, Washington D.C., 1984.

Birdsall, C.K. and Langdon, A.B., *Plasma Physics via Computer Simulation* Plasma Physics Series. IOP Publishing, 1991.

Biskamp, D.: *Nonlinear Magnetohydrodynamics* Cambridge University Press, 1993.

Brackbill, J.U., D.W. Forslund, K.B. Quest, and D. Winske, Nonlinear evolution of the lower-hybrid drift instability, *Phys. Fluids, 27*, 2682, 1984.

Büchner, J., Multiscale coupling in reconnection - Three dimensional current sheet tearing, in *Multiscale coupling in space plasmas*, ed. T. Chang et al., MIT scientific publishers, 79-92, 1995.

Büchner, J., and J.-P. Kuska, Three-dimensional collisionless reconnection through thin current sheets: Theory and selfconsistent simulations in *Third International Conference on Substorms (ICS-3)*, pp. 373, **ESA SP - 389**, October 1996, Noordwijk, The Netherlands, 1996.

Büchner, J., Three-dimensional current sheet tearing in he Earth's magnetotail, *Adv. Space Res.*, 18, 267-272, 1996.

Büchner, J., Transition from Small Scale Turbulence to Large Scale Coherent Reconnection, *Physics of Space Plasmas* 15, 1998

Büchner, J., and J.-P. Kuska, Sausage mode instability of thin current sheets as a cause of magnetospheric substorms, *Ann. Geophys.*, 17, 604-612, 1999.

Büchner, J., Three-dimensional magnetic reconnection in astrophysical plasmas - Kinetic approach, *Astroph. and Space Sci.*, 264, No.1-4, 25-42, 1999.

Galeev, A.A., and L.M. Zelenyi, Tearing instability in plasma configuration, *Sov. Phys. JETP, Engl. Transl., 43*, 1113, 1976.

Harris, E.G., On a plasma sheath separating regions of oppositely directed magnetic field, *Nuovo Cimento*, **23**,115, 1962.

Hesse, M., D. Winske, M. Kuznetsova, Hybrid simulations of collisionless tearing, *J. Geophys. Res., 100*, 18,929, 1995.

Hesse, M., D. Winske, M. Kuznetsova, Electron dissipation in collisionless magnetic reconnection, *J. Geophys. Res., 103*, 26,479, 1998.

Kaufmann, L.R., Substorm currents: Growth phase and onset, *J. Geophys. Res., 92*, 7471, 1987.

Kuska, J.P. and J. Büchner, The three-dimensional fully kinetic electromagnetic PIC simulation code GISMO, in *Proc. VIIth International Conference on Plasma Astrophysics and Space Physics, Kluwer Academic Publishers* 645-52, 1999.

Lembége B. and R. Pellat, Stability of a thick two-dimensional quasi-neutral sheet, *Phys. Fluids, 25*, 1995, 1982.

Lottermoser, R.F. and Scholer, M., Undriven magnetic reconnection in magnetohydrodynamics and Hall magnetohydrodynamics, *J. Geophys. Res., 102*, 4875, 1997.

Mitchell, D.G. et al., Current carriers in the near-Earth's cross-tail current sheet during a substorm growth phase, *Geophys. Res. Lett., 17*, 583, 1990.

Parker, E., *Spontaneous Current Sheets in Magnetic Fields*, Oxford Univ. Press, New York, NY, 1994.

Pritchett, P.L., Effect of electron dynamics on collisionless reconnection in two-dimensional magnetotail equilibria, *J. Geophys. Res., 99*, 9935, 1994.

Pritchett, P.L., and J. Büchner, Collisionless reconnection in configurations with a minimum in the equatorial magnetic field and with magnetic shear, *J. Geophys. Res., 100*, 3601, 1995.

Pritchett, P.L. and F.V. Coroniti, The role of the drift kink mode in destabilizing thin current sheets, *J. Geoelectr., 48*, 833-844, 1996.

Pritchett, P.L., F.V. Coroniti and V.K. Decyk, Three-dimensional stability of thin quasi-neutral current sheets, *J. Geophys. Res., 101*, 27,413, 1996.

Pulkkinen, T., D.N. Baker, R.J. Pellinen, J. Büchner, H.E.J. Koskinen, R.E. Lopez, R.L. Dyson, and L.A. Frank, Particle scattering and current sheet stability in the geomagnetic tail during the substorm growth phase, *J. Geophys. Res., 97*, 19,283, 1992.

Sanny, J., R.L. McPherron, C.T. Russell, D.N. Baker, T.I. Pulkkinen, and A. Nishida, Growth-phase thinning of the near-Earth current sheet during the CDAW 6 substorm, *J. Geophys. Res., 99*, 5805, 1994.

Sergeev, V., et al., Current sheet thickness in the near-Earth plasma sheet during substorm growth phase, *J. Geophys. Res., 95*, 3819, 1990.

Schindler, K., M. Hesse and J. Birn, General reconnection, parallel electric fields and helicity, *J. Geophys. Res., 93*, 5547, 1988.

Schindler, K., and J. Birn, On the cause of thin current sheets in the near-Earth magnetotail and their possible significance for magnetospheric substorms, *J. Geophys. Res., 98*, 15,477, 1993.

Shay, M. A., Drake, J.F., Denton, R.E. and Biskamp, D, Structure of the dissipation region during collisionless magnetic reconnection, *J. Geophys. Res., 103*, 9165, 1998.

Vasyliūnas, V.M., Theoretical models of magnetic field line merging, *Rev. Geophys. Space Phys., 13*, 303, 1975.

Wiegelmann T., and K. Schindler, Formation of thin current sheets in a quasistatic magnetotail model, *Geophys. Res. Lett. 22*, 2057, 1995.

Winske, D., Particle simulation studies of the lower hybrid drift instability, *Phys. Fluids*, *24*, 1069, 1981.

Zhu, Z.W. and R.M. Winglee, Tearing instability, flux ropes, and the kinetic current sheet kink instability in the Earth's magnetotail: A 3-dimensional perspective from particle simulations, *J. Geophys.*, *101*, 4885-4897, 1996.